

---

**Emmanuel Nuño**  
**Luis Basañez**

Institute of Industrial and Control Engineering,  
Technical University of Catalonia,  
Av. Diagonal 647,  
08028 Barcelona,  
Spain  
{emmanuel.nuno, luis.basanez}@upc.edu

**Romeo Ortega**

Laboratoire des Signaux et Systèmes,  
CNRS-SUPÉLEC,  
Plateau de Moulon,  
91190 Gif-sur-Yvette,  
France  
ortega@lss.supelec.fr

**Mark W. Spong**

Erik Jonsson School of Engineering  
and Computer Science,  
University of Texas at Dallas,  
800 West Campbell Road,  
Richardson, TX 75080-3021,  
USA  
mspong@utdallas.edu

# Position Tracking for Non-linear Teleoperators with Variable Time Delay

## Abstract

*In this paper the problem of position tracking in the presence of variable time delay is studied. It is proved that simple P-like and PD-like controllers can stabilize the teleoperator under variable time delays and, moreover, they provide position tracking. Then, a controller based on the scattering transformation that also provides position tracking is proposed. In this paper we present the conditions under which the velocities and position error of the non-linear teleoperator, for the three controllers, are bounded, and if the human does not move the local manipulator and the remote manipulator does not interact with the environment, then it is proved that velocities and position error converge to zero. Simulations and real experiments, using the Internet from Urbana-Champaign (USA) to Barcelona (Spain), validate the proposed schemes.*

KEY WORDS—bilateral teleoperation, time-delays, nonlinear control, internet

## 1. Introduction

In bilateral teleoperation, the local and remote robot manipulators<sup>1</sup> are connected with a communication channel that often involves long distances or imposes limited data transfer between the local and the remote sites. Such situations can result in substantial delays between the time a command is introduced by the operator and the time the command is executed by the remote robot. This time delay effects the overall stability of the system.

Anderson and Spong (1989) have created the basis of *modern* teleoperator control. Their approach was to render passive the communications using the analogy of a lossless transmission line with the scattering theory. They showed that the

---

1. The local and remote manipulators are often called master and slave. However, in bilateral teleoperation the slave influences the master, and it can move according to the slave. Hence, it would be better to call them local and remote robot manipulators or, simply, local and remote.

scattering transformation ensures passivity of the communications despite any constant time delay. Niemeyer and Slotine (1991) introduced the wave variables (scattering transformation), following the former scattering approach, and proved that by matching the impedances of the local and remote robot controllers with the impedance of the *virtual* transmission line, *wave* reflections can be avoided. Those were the beginnings of a series of developments for bilateral teleoperators. The reader may refer to Arcara and Melchiorri (2002) and Hokayem and Spong (2006) for two advanced surveys on this research line. However, the scattering transformation has a tradeoff between stability and performance. In an attempt to improve performance, using the scattering transformation, several approaches have been reported: transmitting *wave* integrals (Ortega et al. 2003; Niemeyer and Slotine 2004; Nufio et al. 2007), *wave* filtering (Tanner and Niemeyer 2005) and *wave* prediction (Munir and Book 2002), amongst others.

It is widely known that using the classic scattering transformation may give raise to position drift. Chopra et al. (2006) achieved position tracking by sending the local position to the remote, and adding a proportional term to the position error in the remote controller. Following this line, Namerikawa and Kawada (2006) proposed a symmetric scheme, by matching the impedances and adding the proportional error term to the local and remote robots, such that the resulting control laws turned into *simple* PD-like controllers. The stability of PD-like controllers, without the scattering transformation, has been proved by Nufio et al. (2008) under the assumption that the human interaction with the local manipulator is passive.

The Internet has become a ubiquitous means of communication, well known for its main applications and protocols e.g. e-mail, www, http, ftp, amongst others. Nevertheless, the use of the Internet, packet switched networks or unreliable communications impose variable time delays and packet loss, and the aforementioned schemes can no longer guarantee a stable behavior under these circumstances (Chopra et al. 2008). In an attempt to provide position tracking under variable time delays, Chopra et al. (2003), with an adaptation of Lozano et al. (2002), have proposed a position drift-free scheme in which the remote robot has a control term that depends on the position error between the local and the remote robots. However, they have not proved the boundedness on the position error; if some velocity restrictions are violated the time derivative of their Lyapunov function loses its non-positiveness property. Moreover, their analysis relies on a linear model of the teleoperator, which is insufficient, in general, for non-linear systems. Hirche and Buss (2004) extended these results analyzing the effects of packet loss in packet switched communication networks, such as the Internet. Munir and Book (2004) used a Kalman filter and a position drift compensator to provide position tracking. Yokokohji et al. (2002) have proposed the use of an energy balance monitor on the local and remote sites to bound the energy increments due to variable time delays, and

with the integral errors of the scattering transformation, they compensate for position drifts.

Motivated by the ubiquitous nature of the Internet, this paper extends the stability results of Nufio et al. (2008) to the variable time delay case and provides some experimental evidence of the achieved performance. In particular, we ensure position tracking capabilities for non-linear teleoperators in the presence of variable time delays on the communication channel. Three controllers that fulfill these conditions are presented, a P-like, a PD-like and a scattering-based controller. It is proved that setting the appropriate control gains, the position error between the local and the remote robots is bounded and, moreover, it asymptotically converges to zero when the operator stands still and the remote manipulator does not interact with the environment. The main contributions of this paper are gathered in Section 3 in Propositions 2–4. In order to prove the effectiveness of the proposed schemes, some simulations and experiments are presented. The experiments have been performed using the Internet, as a communication channel, from Urbana-Champaign (USA) to Barcelona (Spain).

## 2. Preliminaries

Throughout the article we use the following notation:  $\mathbb{R} := (-\infty, \infty)$ ;  $\mathbb{R}^+ := (0, \infty)$ ,  $\mathbb{R}_0^+ := [0, \infty)$ ;  $\lambda_m\{\mathbf{A}\}$  and  $\lambda_M\{\mathbf{A}\}$  represent the minimum and maximum eigenvalue of the positive symmetric matrix  $\mathbf{A}$ , respectively;  $|\cdot|$  stands for the Euclidean norm and  $\|\cdot\|_2$  for the  $\mathcal{L}_2$  norm. In order to keep equations as clear as possible, the argument of all time-dependent signals will be omitted (e.g.  $\dot{\mathbf{q}} \equiv \dot{\mathbf{q}}(t)$ ), except for those which are time delayed (e.g.  $\dot{\mathbf{q}}(t - T)$  for a constant time delay and  $\dot{\mathbf{q}}(t - T(t))$  for a variable time delay). Following this reasoning, the argument of the signals inside the integrals is omitted and it is assumed to be equal to the variable on the differential, unless otherwise stated (e.g.  $\int_0^t \mathbf{x} d\sigma \equiv \int_0^t \mathbf{x}(\sigma) d\sigma$ ).

### 2.1. Modeling the *n*-Degree-of-Freedom Teleoperator System

The local and remote robot manipulators are modeled as a pair of *n*-degree-of-freedom (DOF) serial links with revolute joints. Their corresponding non-linear dynamics are described by

$$\begin{aligned} \mathbf{M}_l(\mathbf{q}_l)\ddot{\mathbf{q}}_l + \mathbf{C}_l(\mathbf{q}_l, \dot{\mathbf{q}}_l)\dot{\mathbf{q}}_l + \mathbf{g}_l(\mathbf{q}_l) &= \boldsymbol{\tau}_l^* - \boldsymbol{\tau}_h \\ \mathbf{M}_r(\mathbf{q}_r)\ddot{\mathbf{q}}_r + \mathbf{C}_r(\mathbf{q}_r, \dot{\mathbf{q}}_r)\dot{\mathbf{q}}_r + \mathbf{g}_r(\mathbf{q}_r) &= \boldsymbol{\tau}_e - \boldsymbol{\tau}_r^*, \end{aligned} \quad (1)$$

where  $\ddot{\mathbf{q}}_i, \dot{\mathbf{q}}_i, \mathbf{q}_i \in \mathbb{R}^n$  are the acceleration, velocity and joint position, respectively,  $\mathbf{M}_i(\mathbf{q}_i) \in \mathbb{R}^{n \times n}$  are the inertia matrices,  $\mathbf{C}_i(\mathbf{q}_i, \dot{\mathbf{q}}_i) \in \mathbb{R}^{n \times n}$  are the Coriolis and centrifugal effects,  $\mathbf{g}_i(\mathbf{q}_i) \in \mathbb{R}^n$  represent the vectors of gravitational forces,  $\boldsymbol{\tau}_i^* \in \mathbb{R}^n$  are the control signals and  $\boldsymbol{\tau}_h \in \mathbb{R}^n$ ,  $\boldsymbol{\tau}_e \in \mathbb{R}^n$  are

the forces exerted by the human operator and the environment interaction, respectively. Here  $i = 1$  represents the local robot and  $i = r$  the remote robot.

These robot dynamic models have some important properties<sup>2</sup> as follows.

P1. Owing to the fact that all joints are revolute, then  $\mathbf{M}_i(\mathbf{q}_i)$  are lower and upper bounded, i.e.

$$0 < \lambda_m\{\mathbf{M}_i(\mathbf{q}_i)\}\mathbf{I} \leq \mathbf{M}_i(\mathbf{q}_i) \leq \lambda_M\{\mathbf{M}_i(\mathbf{q}_i)\}\mathbf{I} < \infty.$$

P2. The Coriolis matrices  $\mathbf{C}_i(\mathbf{q}_i, \dot{\mathbf{q}}_i)$  are given by

$$C_i^{jk}(\mathbf{q}_i, \dot{\mathbf{q}}_i) = \sum_{m=1}^n \frac{1}{2} \underbrace{\left[ \frac{\partial M_i^{jk}}{\partial q_i^m} + \frac{\partial M_i^{jm}}{\partial q_i^k} - \frac{\partial M_i^{km}}{\partial q_i^j} \right]}_{i\Gamma_{km}^j(q_i)} \dot{q}_i^m,$$

where  $i\Gamma_{kl}^j(q_i)$  are the Christoffel symbols of the first kind with the symmetric property that  $i\Gamma_{kl}^j(q_i) = i\Gamma_{lk}^j(q_i)$ . Thus,  $\dot{\mathbf{M}}_i(\mathbf{q}_i) - 2\mathbf{C}_i(\mathbf{q}_i, \dot{\mathbf{q}}_i)$  are skew-symmetric, i.e.

$$\dot{\mathbf{M}}_i(\mathbf{q}_i) = \mathbf{C}_i(\mathbf{q}_i, \dot{\mathbf{q}}_i) + \mathbf{C}_i^T(\mathbf{q}_i, \dot{\mathbf{q}}_i). \quad (2)$$

P3. For all  $\mathbf{q}_i, \mathbf{x}, \mathbf{y} \in \mathbb{R}^n$ , there exists  $k_{c_i} \in \mathbb{R}^+$  such that  $|\mathbf{C}_i(\mathbf{q}_i, \mathbf{x})\mathbf{y}| \leq k_{c_i}|\mathbf{x}||\mathbf{y}|$ . An immediate application is that  $|\mathbf{C}_i(\mathbf{q}_i, \dot{\mathbf{q}})\dot{\mathbf{q}}| \leq k_{c_i}|\dot{\mathbf{q}}|^2$ .

**Proposition 1.** Consider a robot manipulator with only revolute joints of the form (1). Assume that  $\dot{\mathbf{q}}_i, \ddot{\mathbf{q}}_i \in \mathcal{L}_\infty$ , then, the time derivative of its Coriolis matrix  $\dot{\mathbf{C}}_i(\mathbf{q}_i, \dot{\mathbf{q}}_i)$  is bounded.

**Proof.** Proof (Sketch) The elements  $(d/dt)C_i^{jk}(\mathbf{q}_i, \dot{\mathbf{q}}_i)$  are given by combinations of  $\frac{\partial^2 M_i^{jk}(\mathbf{q}_i)}{\partial q_i^j \partial q_i^k}$  (cf. Property P2) which, for manipulators with revolute joints, are products of velocities, accelerations,  $\alpha \sin(\cdot)$  and  $\beta \cos(\cdot)$ .  $\alpha, \beta \in \mathbb{R}^+$  are physical manipulator constants, i.e. the mass distribution and length of the link. Hence, if  $\dot{\mathbf{q}}_i, \ddot{\mathbf{q}}_i \in \mathcal{L}_\infty$  the terms  $\dot{\mathbf{C}}_i(\mathbf{q}_i, \dot{\mathbf{q}}_i)$  are bounded.  $\square$

## 2.2. General Assumptions

We make the following general assumptions.

A1. Following standard considerations, we assume that the human operator and the environment define passive (force to velocity) maps, that is, there exists  $\kappa_i \in \mathbb{R}_0^+$  such that for all  $t \geq 0$ ,

$$\int_0^t \dot{\mathbf{q}}_1^\top \boldsymbol{\tau}_h d\sigma \geq -\kappa_1, \quad -\int_0^t \dot{\mathbf{q}}_r^\top \boldsymbol{\tau}_e d\sigma \geq -\kappa_r. \quad (3)$$

2. The reader may refer to Kelly et al. (2005) and Spong et al. (2005) for a complete guide to the modeling of robot manipulators.

A2. In order to simplify some calculations and to focus on the main idea of this article, we assume that the gravitational forces are precompensated by the controllers  $\boldsymbol{\tau}_i^*$ , (i.e.  $\boldsymbol{\tau}_1^* = \boldsymbol{\tau}_1 + \mathbf{g}_1(\mathbf{q}_1)$  and  $\boldsymbol{\tau}_r^* = \boldsymbol{\tau}_r - \mathbf{g}_r(\mathbf{q}_r)$ ). Hence, the dynamical model (1) changes to

$$\mathbf{M}_1(\mathbf{q}_1)\ddot{\mathbf{q}}_1 + \mathbf{C}_1(\mathbf{q}_1, \dot{\mathbf{q}}_1)\dot{\mathbf{q}}_1 = \boldsymbol{\tau}_1 - \boldsymbol{\tau}_h$$

$$\mathbf{M}_r(\mathbf{q}_r)\ddot{\mathbf{q}}_r + \mathbf{C}_r(\mathbf{q}_r, \dot{\mathbf{q}}_r)\dot{\mathbf{q}}_r = \boldsymbol{\tau}_e - \boldsymbol{\tau}_r. \quad (4)$$

A3. The variable time-delay, that owing to its nature cannot be negative, has a known upper bound  $*T_i$ , i.e.  $0 \leq T_i(t) \leq *T_i < \infty$ .

## 2.3. Instrumental Lemma

The following lemma is an extension for variable time delays of (Nuño et al. 2008, Lemma 1), its proof is presented, for completeness, in Appendix A.

**Lemma 1.** For any vector signals  $\mathbf{x}, \mathbf{y}$ , any variable time delay  $0 \leq T(t) \leq *T < \infty$  and any constant  $\alpha > 0$  we have that

$$\begin{aligned} & -2 \int_0^t \mathbf{x}^\top(\sigma) \int_{-T(\sigma)}^0 \mathbf{y}(\sigma + \theta) d\theta d\sigma \\ & \leq \alpha \|\mathbf{x}\|_2^2 + \frac{*T^2}{\alpha} \|\mathbf{y}\|_2^2. \end{aligned} \quad (5)$$

## 3. Proposed Schemes

This section presents the main contributions of this paper. Three controllers are proposed: a P-like, a PD-like and a scattering-based controller.

### 3.1. P-like Controller

The forces applied by this controller on both the local and the remote manipulators are proportional to their position error plus a damping injection term, see Figure 1.

**Proposition 2.** Consider the teleoperator (4), controlled by

$$\boldsymbol{\tau}_1 = K_1[\mathbf{q}_r(t - T_r(t)) - \mathbf{q}_1] - B_1\dot{\mathbf{q}}_1$$

$$\boldsymbol{\tau}_r = K_r[\mathbf{q}_r - \mathbf{q}_1(t - T_1(t))] + B_r\dot{\mathbf{q}}_r \quad (6)$$

with  $\{K_i, B_i\} \in \mathbb{R}^+$ . Set the control gains such that

$$4B_1B_r > (*T_1^2 + *T_r^2)K_1K_r. \quad (7)$$

Then:

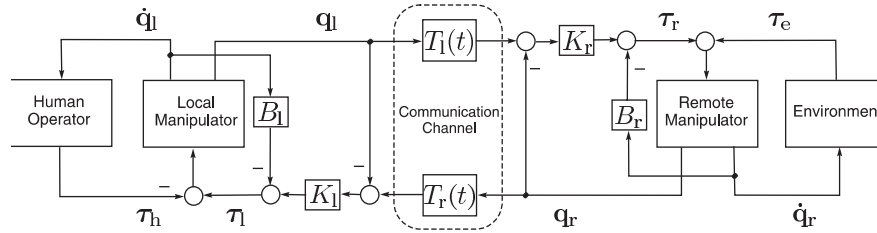


Fig. 1. P-like controller with  $K_i$ ,  $B_i$  the proportional and damping gains, respectively.

- I. Velocities and position error are bounded, i.e.  $\{\dot{\mathbf{q}}_i, \mathbf{q}_i - \mathbf{q}_r\} \in \mathcal{L}_\infty$ ,  $\dot{\mathbf{q}}_i \in \mathcal{L}_2$ , moreover,  $|\mathbf{q}_i - \mathbf{q}_r(t - T_r(t))| \in \mathcal{L}_\infty$ .
- II. In the case that the human does not move the local manipulator and the remote manipulator does not contact the environment (i.e.  $\tau_h = \tau_e = 0$ ), velocities asymptotically converge to zero and position tracking is achieved:

$$|\mathbf{q}_i - \mathbf{q}_r(t - T_r(t))| \rightarrow 0, \quad t \rightarrow \infty.$$

**Proof.** Consider the following Lyapunov function candidate  $V(\mathbf{q}_i, \dot{\mathbf{q}}_i, t)$  given by

$$V = \frac{1}{2} \dot{\mathbf{q}}_i^\top \mathbf{M}_i(\mathbf{q}_i) \dot{\mathbf{q}}_i + \frac{K_1}{2K_r} \dot{\mathbf{q}}_r^\top \mathbf{M}_r(\mathbf{q}_r) \dot{\mathbf{q}}_r + \frac{K_1}{2} |\mathbf{q}_i - \mathbf{q}_r|^2 + \int_0^t \left( \dot{\mathbf{q}}_i^\top \tau_h - \frac{K_1}{K_r} \dot{\mathbf{q}}_r^\top \tau_e \right) d\sigma + \kappa_l + \frac{K_1}{K_r} \kappa_r, \quad (8)$$

Property P1 and Assumption A1 ensure positive-definiteness and radially unboundedness of the Lyapunov function candidate (i.e.  $V > 0$  and  $V \rightarrow \infty$  if  $\{\dot{\mathbf{q}}_i, \mathbf{q}_i\} \rightarrow \infty$ ). The time derivative of (8) along the system trajectories, described by (4) and (6) with Property P3, is given by

$$\begin{aligned} \dot{V} &= -B_l |\dot{\mathbf{q}}_l|^2 - \frac{K_1 B_r}{K_r} |\dot{\mathbf{q}}_r|^2 + K_1 \dot{\mathbf{q}}_l^\top [\mathbf{q}_r(t - T_r(t)) - \mathbf{q}_r] \\ &+ K_1 \dot{\mathbf{q}}_r^\top [\mathbf{q}_l(t - T_l(t)) - \mathbf{q}_l] \end{aligned} \quad (9)$$

taking the terms in brackets, we can show that

$$\mathbf{q}_i(t - T_i(t)) - \mathbf{q}_i = - \int_{-T_i(t)}^0 \dot{\mathbf{q}}_i(t + \theta) d\theta. \quad (10)$$

We can recover the original signals with a simple analysis:

$$\dot{\mathbf{q}}_i(t + \theta) = \frac{d\mathbf{q}_i(t + \theta)}{d(t + \theta)}$$

and

$$\frac{d(t + \theta)}{d\theta} = 1,$$

hence,

$$\dot{\mathbf{q}}_i(t + \theta) = \frac{d\mathbf{q}_i(t + \theta)}{d(t + \theta)} \frac{d(t + \theta)}{d\theta} = \frac{d\mathbf{q}_i(t + \theta)}{d\theta},$$

thus

$$\begin{aligned} - \int_{-T_i(t)}^0 \dot{\mathbf{q}}_i(t + \theta) d\theta &= - \int_{-T_i(t)}^0 \frac{d\mathbf{q}_i(t + \theta)}{d\theta} d\theta \\ &= -\mathbf{q}_i(t + \theta) \Big|_{\theta=-T_i(t)}^{\theta=0}. \end{aligned}$$

Rewriting (9) with these new transformations we obtain

$$\begin{aligned} \dot{V} &= -B_l |\dot{\mathbf{q}}_l|^2 - \frac{K_1 B_r}{K_r} |\dot{\mathbf{q}}_r|^2 - K_1 \dot{\mathbf{q}}_l^\top \int_{-T_r(t)}^0 \dot{\mathbf{q}}_r(t + \theta) d\theta \\ &- K_1 \dot{\mathbf{q}}_r^\top \int_{-T_l(t)}^0 \dot{\mathbf{q}}_l(t + \theta) d\theta. \end{aligned}$$

Integrating from zero to  $t$ , and invoking Lemma 1 on the last two terms on the right-hand side with  $\alpha_l$  and  $\alpha_r$ , respectively, yields

$$\begin{aligned} V(t) - V(0) &\leq - \left[ B_l - \frac{K_1}{2} \left( \alpha_l + \frac{{}^*T_l^2}{\alpha_r} \right) \right] \|\dot{\mathbf{q}}_l\|_2^2 \\ &- \left[ \frac{K_1 B_r}{K_r} - \frac{K_1}{2} \left( \alpha_r + \frac{{}^*T_r^2}{\alpha_l} \right) \right] \|\dot{\mathbf{q}}_r\|_2^2. \end{aligned} \quad (11)$$

Take

$$\lambda_l = B_l - \frac{K_1}{2} \left( \alpha_l + \frac{{}^*T_l^2}{\alpha_r} \right)$$

and

$$\lambda_r = B_r - \frac{K_r}{2} \left( \alpha_r + \frac{{}^*T_r^2}{\alpha_l} \right),$$

if there exists  $\lambda_i > 0$ , then

$$-V(0) \leq -\lambda_l \|\dot{\mathbf{q}}_l\|_2^2 - \lambda_r \|\dot{\mathbf{q}}_r\|_2^2,$$

thus  $\{\dot{\mathbf{q}}_l, \dot{\mathbf{q}}_r\} \in \mathcal{L}_2$ . Solving simultaneously for  $\lambda_i > 0$  and  $\alpha_i > 0$ , one obtains

$$\frac{2B_r}{K_r} - \frac{{}^*T_r^2}{\alpha_l} > \alpha_r > \frac{{}^*T_l^2 K_1}{2B_l + K_1 \alpha_l},$$

after a little manipulation, while solving for  $\alpha_l > 0$ , the following inequality arises

$$(4B_l B_r - {}^*T_l^2 K_1 K_r - {}^*T_r^2 K_1 K_r) \alpha_l + 2B_r K_1 \alpha_l^2 + 2{}^*T_r^2 B_l K_l > 0$$

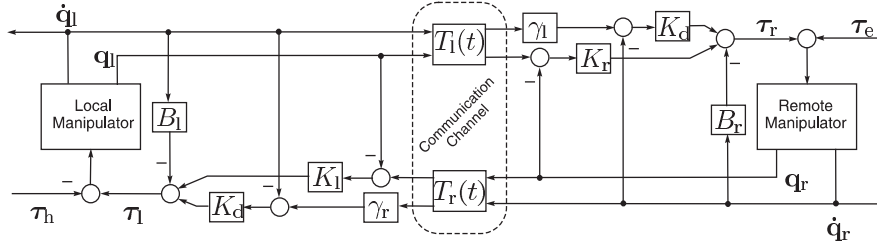


Fig. 2. PD-like controller with  $K_i$ ,  $K_d$ ,  $B_i$  the P, D and damping gains. Here  $\gamma_i$  are time-varying gains.

which, for  $\alpha_1 > 0$  has a solution if  $4B_l B_r > (*T_l^2 + *T_r^2)K_l K_r$ . Then, setting the control gains fulfilling this last inequality ensures that there exists  $\alpha_i > 0$  such that  $\lambda_i > 0$ , thus  $\dot{q}_i \in \mathcal{L}_2$ . This fact, together with Property P1, implies that  $V(t) \leq V(0)$ , thus (8) is bounded. Hence,  $\{\dot{q}_l, \dot{q}_r, q_l - q_r\} \in \mathcal{L}_\infty$ .

Rewriting  $q_l - q_r(t - T_r(t))$  as

$$q_l - q_r(t - T_r(t)) = \underbrace{q_l - q_r}_{\mathcal{L}_\infty} + q_r - q_r(t - T_r(t))$$

and the fact that  $q_r - q_r(t - T_r(t)) = \int_0^{T_r(t)} \dot{q}_r(t - \theta) d\theta \leq *T_r^{\frac{1}{2}} \|\dot{q}_r\|_2$  (using Schwartz's inequality), we conclude that  $q_l - q_r(t - T_r(t)) \in \mathcal{L}_\infty$ . In the same manner we can prove that  $q_r - q_l(t - T_l(t)) \in \mathcal{L}_\infty$ . This completes the first part of the proof.

The outline of the second part of the proof is as follows: first it is proved that when  $\tau_h = \tau_e = 0$ , velocities converge to zero; then, the zero-convergence of accelerations is proved. Finally, the proof of position coordination is straightforward.

Let us rewrite (4), with the controllers (6) and  $\tau_h = \tau_e = 0$ , as

$$\begin{aligned} \ddot{q}_l &= -M_l^{-1}(q_l)[K_l[q_l - q_r(t - T_r(t))] \\ &\quad + B_l \dot{q}_l + C_l(q_l, \dot{q}_l)\dot{q}_l] \\ \ddot{q}_r &= -M_r^{-1}(q_r)[K_r[q_r - q_l(t - T_l(t))] \\ &\quad + B_r \dot{q}_r + C_r(q_r, \dot{q}_r)\dot{q}_r] \end{aligned} \quad (12)$$

The fact that  $\{\dot{q}_i, q_l - q_r(t - T_r(t)), q_r - q_l(t - T_l(t))\} \in \mathcal{L}_\infty$ , together with Properties P1 and P3, allow us to conclude that  $\ddot{q}_i \in \mathcal{L}_\infty$ . Hence, Barbălat's lemma guarantees that  $\dot{q}_i \rightarrow 0$  as  $t \rightarrow \infty$ , because  $\dot{q}_i \in \mathcal{L}_\infty$  and  $\dot{q}_i \in \mathcal{L}_\infty \cap \mathcal{L}_2$ .

From (12) it can be easily seen that position tracking will be established if we prove that  $\ddot{q}_i \rightarrow 0$  when  $\dot{q}_i \rightarrow 0$ . Differentiating (12) we obtain two types of terms: one consisting of  $(d/dt)M_i^{-1}(q_i)$  times a bounded signal and, the other, the product of  $M_i^{-1}(q_i)$  times the derivative of the term in brackets. For the first term we have

$$\frac{d}{dt}M_i^{-1} = -M_i^{-1}\dot{M}_i M_i^{-1} = -M_i^{-1}(C_i + C_i^T)M_i^{-1},$$

which is clearly bounded because of Properties P1 and P3. The derivative of the term in brackets in (12), is bounded because it is a sum of bounded elements (Proposition 1 shows that, when  $\{\dot{q}_i, \ddot{q}_i\} \in \mathcal{L}_\infty$ ,  $\dot{C}_i(q_i, \dot{q}_i)$  are bounded). Consequently,  $(d/dt)\ddot{q}_i \in \mathcal{L}_\infty$ , thus  $\ddot{q}_i$  are uniformly continuous. Using Barbălat's lemma, we conclude that  $\ddot{q}_i \rightarrow 0$ . Hence, when  $\dot{q}_i \rightarrow 0$  then  $\ddot{q}_i \rightarrow 0$  as required. Thus,

$$\lim_{t \rightarrow \infty} |q_l - q_r(t - T_r(t))| = 0.$$

This completes the proof.  $\square$

### 3.2. PD-like Controller

The PD-like control laws are given by

$$\begin{aligned} \tau_l &= K_d[\gamma_l \dot{q}_r(t - T_r(t)) - \dot{q}_l] \\ &\quad + K_l[q_r(t - T_r(t)) - q_l] + B_l \dot{q}_l \\ \tau_r &= K_d[\dot{q}_r - \gamma_r \dot{q}_l(t - T_l(t))] \\ &\quad + K_r[q_r - q_l(t - T_l(t))] + B_r \dot{q}_r \end{aligned} \quad (13)$$

with  $\{K_i, K_d, B_i\} \in \mathbb{R}^+$  and  $\gamma_i^2 = 1 - \dot{T}_i(t)$ . If time delays increase or decrease, then the time-varying gains  $\gamma_i$  dissipate the energy generated by the communications; this fact can be observed from the last two terms in the Lyapunov-like function (14) and their derivatives in (15). Figure 2 depicts the block diagram of these controllers.

**Proposition 3.** Consider the teleoperator (4), controlled by (13). Set the control gains  $B_r \geq B_l$  and  $K_r \geq K_l$  fulfilling (7). In addition assume that time delays do not grow or decrease faster than time itself, i.e.  $|\dot{T}_i(t)| < 1$ . Then, Proposition 2 holds if the controllers (6) are changed for (13) with any arbitrary positive  $K_d$ .  $\square$

**Proof.** Let us propose the following positive-definite and radially unbounded Lyapunov–Krasovskii function candidate

$$\begin{aligned}
V &= \frac{1}{2} \dot{\mathbf{q}}_l^\top \mathbf{M}_l(\mathbf{q}_l) \dot{\mathbf{q}}_l + \frac{K_l}{2K_r} \dot{\mathbf{q}}_r^\top \mathbf{M}_r(\mathbf{q}_r) \dot{\mathbf{q}}_r + \frac{K_l}{2} |\mathbf{q}_l - \mathbf{q}_r|^2 \\
&+ \int_0^t \left( \dot{\mathbf{q}}_l^\top \boldsymbol{\tau}_h - \frac{K_l}{K_r} \dot{\mathbf{q}}_r^\top \boldsymbol{\tau}_e \right) d\sigma + \kappa_l + \frac{K_l}{K_r} \kappa_r \\
&+ \frac{K_d K_l}{2K_r} \int_{t-T_l(t)}^t |\dot{\mathbf{q}}_l(\theta)|^2 d\theta \\
&+ \frac{K_d}{2} \int_{t-T_r(t)}^t |\dot{\mathbf{q}}_r(\theta)|^2 d\theta, \quad (14)
\end{aligned}$$

its time derivative along the system trajectories described by (4) with Property P3 of the robot manipulators yields

$$\begin{aligned}
\dot{V} &= \dot{\mathbf{q}}_l^\top \boldsymbol{\tau}_l - \frac{K_l}{K_r} \dot{\mathbf{q}}_r^\top \boldsymbol{\tau}_r + K_l [\mathbf{q}_l - \mathbf{q}_r]^\top [\dot{\mathbf{q}}_l - \dot{\mathbf{q}}_r] \\
&+ \frac{K_d K_l}{2K_r} [|\dot{\mathbf{q}}_l|^2 - \gamma_l^2 |\dot{\mathbf{q}}_l(t - T_l(t))|^2] \\
&+ \frac{K_d}{2} [|\dot{\mathbf{q}}_r|^2 - \gamma_r^2 |\dot{\mathbf{q}}_r(t - T_r(t))|^2], \quad (15)
\end{aligned}$$

where  $\gamma_i^2 = 1 - \dot{T}_i(t)$ . Substituting the control laws given by (13), using (10), and the bounds

$$2\dot{\mathbf{q}}_l^\top \gamma_r \dot{\mathbf{q}}_r(t - T_r(t)) \leq |\dot{\mathbf{q}}_l|^2 + \gamma_r^2 |\dot{\mathbf{q}}_r(t - T_r(t))|^2$$

and

$$2\dot{\mathbf{q}}_r^\top \gamma_l \dot{\mathbf{q}}_l(t - T_l(t)) \leq |\dot{\mathbf{q}}_r|^2 + \gamma_l^2 |\dot{\mathbf{q}}_l(t - T_l(t))|^2,$$

we get

$$\begin{aligned}
\dot{V} &\leq - \left[ B_l - \frac{K_d}{2} \left( \frac{K_l}{K_r} - 1 \right) \right] |\dot{\mathbf{q}}_l|^2 \\
&- K_l \dot{\mathbf{q}}_l^\top \int_{-T_r(t)}^0 \dot{\mathbf{q}}_r(t + \theta) d\theta \\
&- \left[ B_r - \frac{K_d}{2} \left( \frac{K_l}{K_r} - 1 \right) \right] |\dot{\mathbf{q}}_r|^2 \\
&- K_l \dot{\mathbf{q}}_r^\top \int_{-T_l(t)}^0 \dot{\mathbf{q}}_l(t + \theta) d\theta. \quad (16)
\end{aligned}$$

Integrating from zero to  $t$  and applying Lemma 1 to the integral signals with  $\alpha_l$  and  $\alpha_r$ , respectively, yields

$$V(t) - V(0) \leq -\lambda_l \|\dot{\mathbf{q}}_l\|_2^2 - \lambda_r \|\dot{\mathbf{q}}_r\|_2^2, \quad (17)$$

with

$$\begin{aligned}
\lambda_l &= \left[ B_l - \frac{K_d}{2} \left( \frac{K_l}{K_r} - 1 \right) - \frac{K_l}{2} \left( \alpha_l + \frac{{}^*T_l^2}{\alpha_r} \right) \right] \\
\lambda_r &= \left[ \frac{K_l B_r}{K_r} - \frac{K_d}{2} \left( \frac{K_l}{K_r} - 1 \right) - \frac{K_l}{2} \left( \alpha_r + \frac{{}^*T_r^2}{\alpha_l} \right) \right]
\end{aligned}$$

If there exists  $\lambda_i > 0$  and  $\alpha_i > 0$ , then  $\dot{\mathbf{q}}_i \in \mathcal{L}_2$ .

Note that if  $K_r = K_l$ , the rest of the proof follows *verbatim* the proof of Proposition 2. Otherwise, solving simultaneously for  $\lambda_i > 0$ ,  $\alpha_i > 0$ , and after some manipulations, one obtains

$$\begin{aligned}
&4B_l B_r + \frac{2K_l B_r K_d}{K_r} + 2K_d [B_r - B_l] + \frac{2B_l K_r K_d}{K_l} \\
&+ K_d^2 \left[ \frac{K_r}{K_l} - \frac{K_l}{K_r} \right] - K_l K_r [{}^*T_l^2 + {}^*T_r^2] > 0
\end{aligned}$$

which for any arbitrary positive  $K_d$ ,  $K_r \geq K_l$  and  $B_r \geq B_l$ , there will exist a positive solution for  $\lambda_i$  and  $\alpha_i$  if

$$4B_l B_r > ({}^*T_l^2 + {}^*T_r^2) K_l K_r.$$

The rest of the proof follows *verbatim* the steps of the proof of Proposition 2 with the assumption that  $|\dot{T}_i(t)| < 1$ , which allows one to show that  $0 < \gamma_i < \sqrt{2}$ , ensuring that

$$\dot{\gamma}_i(t) = \frac{-\ddot{T}_i(t)}{[1 - \dot{T}_i(t)]^{\frac{1}{2}}}$$

is bounded.  $\square$

### 3.3. Scattering Transformation for Variable Time Delays

Anderson and Spong (1989) established the basis for the scattering transformation (wave variables) of Niemeyer and Slotine (1991). This transformation is given by

$$\begin{aligned}
\mathbf{u}_l &= \frac{1}{\sqrt{2b}} (\boldsymbol{\tau}_{ld} - b\dot{\mathbf{q}}_{ld}), & \mathbf{u}_r &= \frac{1}{\sqrt{2b}} (\boldsymbol{\tau}_{rd} - b\dot{\mathbf{q}}_{rd}), \\
\mathbf{v}_l &= \frac{1}{\sqrt{2b}} (\boldsymbol{\tau}_{ld} + b\dot{\mathbf{q}}_{ld}), & \mathbf{v}_r &= \frac{1}{\sqrt{2b}} (\boldsymbol{\tau}_{rd} + b\dot{\mathbf{q}}_{rd}), \quad (18)
\end{aligned}$$

where  $b$  is the *virtual* impedance of the transmission line and the subscript  $id$ , where  $i = l, r$ , means local or remote desired signals, respectively. The reader may refer to Rinaldis et al. (2006) for the application of the dual idea, that is, transform a real transmission line into pure delays.

The local and the remote manipulators are interconnected, for constant time delays in the forward and the backward paths ( $T_l$  and  $T_r$ , respectively), as

$$\mathbf{u}_l = \mathbf{u}_r(t - T_l), \quad \mathbf{v}_l = \mathbf{v}_r(t - T_r). \quad (19)$$

Using these transformations, (18) and (19), it has been shown that the total energy in the communications is stored within signal transmissions as

$$E_{\text{comm}} = \frac{1}{2} \int_{t-T_l}^t |\mathbf{u}_l|^2 d\sigma + \frac{1}{2} \int_{t-T_r}^t |\mathbf{v}_r|^2 d\sigma \geq 0, \quad (20)$$

which means that the communications are passive independent of the magnitude of the constant time delay. However, it has



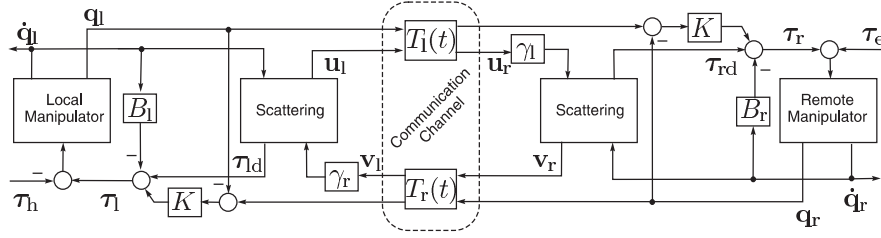


Fig. 3. Scattering-based controller for variable time delays.

been shown, by Lozano et al. (2002), that in the presence of variable time delays  $T_i(t)$  this statement no longer applies, and the communications are, in general, not passive. In order to render passive these communications, it has been suggested, by Lozano et al. (2002), the use of a time-varying gain  $\gamma_i$  in the local and remote interconnection, given by

$$\mathbf{u}_r = \gamma_l \mathbf{u}_l(t - T_l(t)), \quad \mathbf{v}_l = \gamma_r \mathbf{v}_r(t - T_r(t)), \quad (21)$$

where  $\gamma_i^2 \leq 1 - \dot{T}_i(t)$ . This, together with (18), provides a positive-definite energy storage function for the communications, which is given by

$$\begin{aligned} E_{\text{comm}} &= \frac{1}{2} \int_{t-T_l(t)}^t |\mathbf{u}_l|^2 d\sigma \\ &+ \frac{1 - \dot{T}_l(t) - \gamma_l^2}{2 - 2\dot{T}_l(t)} \int_0^{t-T_l(t)} |\mathbf{u}_l|^2 d\sigma \\ &+ \frac{1}{2} \int_{t-T_r(t)}^t |\mathbf{v}_r|^2 d\sigma \\ &+ \frac{1 - \dot{T}_r(t) - \gamma_r^2}{2 - 2\dot{T}_r(t)} \int_0^{t-T_r(t)} |\mathbf{v}_r|^2 d\sigma. \end{aligned} \quad (22)$$

This means that by choosing an appropriate  $\gamma_i$ , the communications do not generate energy. Note that if  $\gamma_i^2 = 1 - \dot{T}_i(t)$ , (22) becomes an expression like (20).

In order to provide position tracking capabilities for variable time delays, Chopra et al. (2003) have added a control term on the remote controller such that

$$\tau_r = \tau_{rd} + K \text{sat}_p(\mathbf{e}) + B_l \dot{\mathbf{q}}_l,$$

where  $\mathbf{e}$  is the teleoperator position error given by  $\mathbf{e} = \dot{\mathbf{q}}_r - \dot{\mathbf{q}}_l(t - T_l(t))$ , and  $\text{sat}_p(\mathbf{e})$  is a vector defined as

$$\text{sat}_p(\mathbf{e}) = \begin{cases} \mathbf{e} & |\mathbf{e}| \leq p, \\ p \frac{\mathbf{e}}{|\mathbf{e}|} & |\mathbf{e}| > p. \end{cases}$$

Nevertheless, they did not prove boundedness of the tracking error, moreover the stability is compromised if  $|\dot{\mathbf{q}}_l| \geq (p/\sqrt{2B_l})$ ,  $|\dot{\mathbf{q}}_r| \geq (p/\sqrt{2B_r - K^2})$  or  $|\dot{\mathbf{q}}_r - \dot{\mathbf{q}}_{rd}| \geq (p/\sqrt{2B_r})$ .

This means that if  $\dot{\mathbf{q}}_i, \dot{\mathbf{q}}_{rd} \rightarrow 0$  their Lyapunov function cannot guarantee stability. In order to cope with this problem they have analyzed the linearized model of (4) and showed that all solutions of this linearized model with initial conditions satisfying a certain bound will remain bounded. However this is, in general, not true for non-linear systems.

In this article we prove that it is indeed possible to achieve position tracking for variable time delays using the scattering transformation. The proposed scheme is depicted in Figure 3, for which the controllers are given by

$$\begin{aligned} \tau_l &= \tau_{ld} + K[\mathbf{q}_r(t - T_r(t)) - \mathbf{q}_l] - B_l \dot{\mathbf{q}}_l, \\ \tau_r &= \tau_{rd} + K[\mathbf{q}_r - \mathbf{q}_l(t - T_l(t))] + B_r \dot{\mathbf{q}}_r, \end{aligned} \quad (23)$$

where

$$\begin{aligned} \tau_{ld} &= -K_{dl}[\dot{\mathbf{q}}_l - \dot{\mathbf{q}}_{ld}] \\ \tau_{rd} &= K_{dr}[\dot{\mathbf{q}}_r - \dot{\mathbf{q}}_{rd}], \end{aligned} \quad (24)$$

and the desired velocities are codified using (18) and (21) with  $\gamma_i^2 = 1 - \dot{T}_i(t)$ .

**Proposition 4.** *Proposition 2 holds if the controllers (6) are replaced by (23)–(24) with  $\{K, K_{di}, B_i\} \in \mathbb{R}^+$  satisfying (7). Using the scattering transformation given by (18) and (21) with  $\gamma_i^2 = 1 - \dot{T}_i(t)$ . Under the additional assumption that  $|\dot{T}_i(t)| < 1$ .*

**Proof.** Let us propose the following Lyapunov function candidate  $V(\mathbf{q}_i, \dot{\mathbf{q}}_i, t)$  given by

$$\begin{aligned} V &= \frac{1}{2} \dot{\mathbf{q}}_l^\top \mathbf{M}_l(\mathbf{q}_l) \dot{\mathbf{q}}_l + \frac{1}{2} \dot{\mathbf{q}}_r^\top \mathbf{M}_r(\mathbf{q}_r) \dot{\mathbf{q}}_r + \frac{1}{2} K |\mathbf{q}_l - \mathbf{q}_r|^2 \\ &+ \int_0^t (\dot{\mathbf{q}}_l^\top \tau_h - \dot{\mathbf{q}}_r^\top \tau_e) d\sigma + \kappa_l + \kappa_r \\ &+ \int_0^t (\dot{\mathbf{q}}_{rd}^\top \tau_{rd} - \dot{\mathbf{q}}_{ld}^\top \tau_{ld}) d\sigma, \end{aligned} \quad (25)$$

using (18) and (21) with  $\gamma_i^2 = 1 - \dot{T}_i(t)$ , it can be seen, from (22), that

$$\begin{aligned} & \int_0^t (\dot{\mathbf{q}}_{rd}^\top \boldsymbol{\tau}_{rd} - \dot{\mathbf{q}}_{ld}^\top \boldsymbol{\tau}_{ld}) d\sigma \\ &= \frac{1}{2} \int_{t-T_l(t)}^t |\mathbf{u}_l|^2 d\sigma + \frac{1}{2} \int_{t-T_r(t)}^t |\mathbf{v}_r|^2 d\sigma \geq 0, \end{aligned}$$

this, together with Assumption A1 and Property P1, show that (25) is positive definite and radially unbounded for variable time delays.

The time derivative of (25) along the system trajectories, described by (4), (23) and (24), and the Property P3, is given by

$$\begin{aligned} \dot{V} &= -B_l |\dot{\mathbf{q}}_l|^2 - B_r |\dot{\mathbf{q}}_r|^2 - K_{dl} |\dot{\mathbf{q}}_l - \dot{\mathbf{q}}_{ld}|^2 - K_{dr} |\dot{\mathbf{q}}_r - \dot{\mathbf{q}}_{rd}|^2 \\ &+ K \dot{\mathbf{q}}_l^\top [\mathbf{q}_r(t - T_r(t)) - \mathbf{q}_r] + K \dot{\mathbf{q}}_r^\top [\mathbf{q}_l(t - T_l(t)) - \mathbf{q}_l], \end{aligned}$$

using the transformations (10), we obtain

$$\begin{aligned} \dot{V} &= -B_l |\dot{\mathbf{q}}_l|^2 - B_r |\dot{\mathbf{q}}_r|^2 - K_{dl} |\dot{\mathbf{q}}_l - \dot{\mathbf{q}}_{ld}|^2 - K_{dr} |\dot{\mathbf{q}}_r - \dot{\mathbf{q}}_{rd}|^2 \\ &- K \dot{\mathbf{q}}_l^\top \int_{-T_r(t)}^0 \dot{\mathbf{q}}_r(t + \theta) d\theta - K \dot{\mathbf{q}}_r^\top \int_{-T_l(t)}^0 \dot{\mathbf{q}}_l(t + \theta) d\theta. \end{aligned}$$

Integrating from zero to  $t$ , and applying Lemma 1 to the last two terms, yields

$$\begin{aligned} & V(t) - V(0) \\ &\leq - \left[ B_l - \frac{K}{2} \left( \alpha_1 + \frac{*T_l^2}{\alpha_r} \right) \right] \|\dot{\mathbf{q}}_l\|_2^2 - K_{dl} \|\dot{\mathbf{q}}_l - \dot{\mathbf{q}}_{ld}\|_2^2 \\ &- \left[ B_r - \frac{K}{2} \left( \alpha_r + \frac{*T_r^2}{\alpha_l} \right) \right] \|\dot{\mathbf{q}}_r\|_2^2 - K_{dr} \|\dot{\mathbf{q}}_r - \dot{\mathbf{q}}_{rd}\|_2^2, \end{aligned}$$

which is noting but (11), hence, if (7) holds, then  $\dot{\mathbf{q}}_i \in \mathcal{L}_2 \cap \mathcal{L}_\infty$  and  $\mathbf{q}_l - \mathbf{q}_r \in \mathcal{L}_\infty$ . This completes the first part of the proof.

In order to establish the second part, we have to prove that  $\boldsymbol{\tau}_i \in \mathcal{L}_\infty$  given by (23), which can be established if  $\dot{\mathbf{q}}_{id} \in \mathcal{L}_\infty$ . Taking (18), (21) and (24), the desired velocities become

$$\begin{aligned} \dot{\mathbf{q}}_{ld} &= \frac{1}{b + K_{dl}} [K_{dl} \dot{\mathbf{q}}_l + \gamma_r K_{dr} \dot{\mathbf{q}}_r(t - T_r(t)) \\ &+ \gamma_l [b - K_{dr}] \dot{\mathbf{q}}_{rd}(t - T_r(t))], \\ \dot{\mathbf{q}}_{rd} &= \frac{1}{b + K_{dr}} [K_{dr} \dot{\mathbf{q}}_r + \gamma_l K_{dl} \dot{\mathbf{q}}_l(t - T_l(t)) \\ &+ \gamma_r [b - K_{dl}] \dot{\mathbf{q}}_{ld}(t - T_l(t))]. \end{aligned}$$

These difference equations are stable if  $\dot{T}_i(t) \leq 1$ . Thus,  $\dot{\mathbf{q}}_{id} \in \mathcal{L}_\infty$ , which guarantees that  $\boldsymbol{\tau}_i \in \mathcal{L}_\infty$ , the assumption that  $|\dot{T}_i(t)| < 1$  ensures that  $\gamma_i$  is bounded. The rest the proof follows *verbatim* the second part of the proof of Proposition 2.

**Remark 1.** Performance of the scattering-based controller of Proposition 4 is improved using the impedance matching of Niemeyer and Slotine (2004). Choose  $K_{dl} = K_{dr} = b$ , then the desired velocities become

$$\begin{aligned} \dot{\mathbf{q}}_{ld} &= \frac{1}{2} [\dot{\mathbf{q}}_l + \gamma_r \dot{\mathbf{q}}_r(t - T_r(t))] \\ \dot{\mathbf{q}}_{rd} &= \frac{1}{2} [\dot{\mathbf{q}}_r + \gamma_l \dot{\mathbf{q}}_l(t - T_l(t))] \end{aligned}$$

and, substituting them on the control laws (23) yields

$$\begin{aligned} \boldsymbol{\tau}_l &= \frac{b}{2} [\gamma_r \dot{\mathbf{q}}_r(t - T_r(t)) - \dot{\mathbf{q}}_r] \\ &+ K [\mathbf{q}_r(t - T_r(t)) - \mathbf{q}_l] - B_l \dot{\mathbf{q}}_l \end{aligned} \quad (26)$$

$$\begin{aligned} \boldsymbol{\tau}_r &= \frac{b}{2} [\dot{\mathbf{q}}_r - \gamma_l \dot{\mathbf{q}}_l(t - T_l(t))] \\ &+ K [\mathbf{q}_r - \mathbf{q}_l(t - T_l(t))] + B_r \dot{\mathbf{q}}_r \end{aligned} \quad (27)$$

which is nothing but the *simple* PD-like controller for variable time delays, analyzed in Proposition 3.

The following proposition is a comment on the transparency of the proposed schemes.

**Proposition 5.** Consider the teleoperator (4), controlled by (6) with  $K_i = K$ , (13) with  $K_i = K$  or (23) for any arbitrary positive  $K$ . Then, in steady state (i.e.  $\ddot{\mathbf{q}}_i = \dot{\mathbf{q}}_i = 0$ ), the human operator feels what the remote manipulator is touching (i.e.  $\boldsymbol{\tau}_h = \boldsymbol{\tau}_e$ ).

**Proof.** This proposition is easily established if we rewrite the teleoperator dynamics (4) with each controller (6), (13) or (23) in steady state as

$$\boldsymbol{\tau}_h = K [\mathbf{q}_r - \mathbf{q}_l] = \boldsymbol{\tau}_e.$$

□

## 4. Simulations

In order to show the effectiveness of the proposed schemes, this section presents simulations of the teleoperators in closed loop with the P-like (Proposition 2) and the PD-like (Proposition 3) controllers. Simulation results of the scattering-based controller are omitted, owing to the exact behavior of the scattering-based and the PD-like controller, see Remark 1.

The local and remote manipulators are modeled as a pair of 2-DOF serial links with revolute joints (see Figure 4). Their corresponding non-linear dynamics follow (1). The inertia matrix  $\mathbf{M}_i(\mathbf{q}_i)$  is given by

$$\mathbf{M}_i(\mathbf{q}_i) = \begin{bmatrix} \alpha_i + 2\beta_i \cos(q_{2i}) & \delta_i + \beta_i \cos(q_{2i}) \\ \delta_i + \beta_i \cos(q_{2i}) & \delta_i \end{bmatrix}. \quad (28)$$



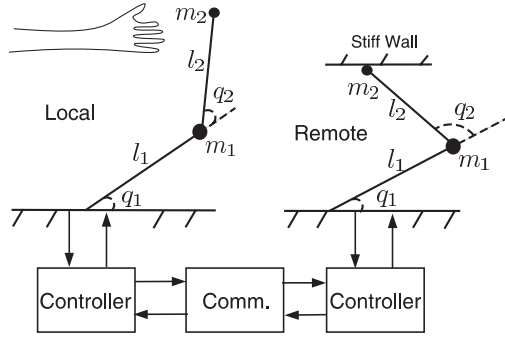


Fig. 4. Simulations scheme.

Here  $q_{k_i}$  is the articular position of each link with  $k \in \{1, 2\}$ ,  $\alpha_i = l_{2_i}^2 m_{2_i} + l_{1_i}^2 (m_{1_i} + m_{2_i})$ ,  $\beta_i = l_{1_i} l_{2_i} m_{2_i}$  and  $\delta_i = l_{2_i}^2 m_{2_i}$ . The lengths for both links  $l_{1_i}$  and  $l_{2_i}$ , in each manipulator, are 0.38 m. The masses for each link correspond to  $m_{1_l} = 3.9473$  kg,  $m_{2_l} = 0.6232$  kg,  $m_{1_r} = 3.2409$  kg and  $m_{2_r} = 0.3185$  kg, respectively. These values are the same as those used by Lee and Spong (2006). Coriolis and centrifugal forces are modeled as the vector  $C_i(\mathbf{q}_i, \dot{\mathbf{q}}_i)\dot{\mathbf{q}}_i$  which are

$$C_i(\mathbf{q}_i, \dot{\mathbf{q}}_i)\dot{\mathbf{q}}_i = \begin{bmatrix} -\beta_i \sin(q_{2_i}) \dot{q}_{2_i}^2 - \beta_i \sin(q_{2_i}) \dot{q}_{1_i} \dot{q}_{2_i} \\ \beta_i \sin(q_{2_i}) \dot{q}_{1_i}^2 \end{bmatrix},$$

where  $\dot{q}_{1_i}$  and  $\dot{q}_{2_i}$  are the respective revolute velocities of the two links. The gravity effects for each manipulator are represented by

$$\mathbf{g}_i(\mathbf{q}_i) = \begin{bmatrix} \frac{1}{l_{2_i}} g \delta_i \cos(q_{1_i} + q_{2_i}) + \frac{1}{l_{1_i}} (\alpha_i - \delta_i) \cos(q_{1_i}) \\ \frac{1}{l_{2_i}} g \delta_i \cos(q_{1_i} + q_{2_i}) \end{bmatrix}.$$

At this point, we should clarify that the human exerts a force on the local manipulator's tip, and the remote manipulator interaction with the environment is also measured at its tip. Hence, for the simulations the following expressions are used  $\tau_h = \mathbf{J}_l^T(\mathbf{q}_l)\mathbf{f}_h$  and  $\tau_e = \mathbf{J}_r^T(\mathbf{q}_r)\mathbf{f}_e$ , ( $\mathbf{J}_i^T(\mathbf{q}_i)$  is the Jacobian transposed of the robot manipulator). The Jacobians take the following expression

$$\mathbf{J}_i(\mathbf{q}_i) = \begin{bmatrix} -l_{1_i} \sin(q_{1_i}) - l_{2_i} \sin(q_{1_i} + q_{2_i}) & -l_{2_i} \sin(q_{1_i} + q_{2_i}) \\ l_{1_i} \cos(q_{1_i}) + l_{2_i} \cos(q_{1_i} + q_{2_i}) & l_{2_i} \cos(q_{1_i} + q_{2_i}) \end{bmatrix}.$$

For simplicity the variable time delays are the same for both, forward and backward paths. Figure 5 shows a sinusoidal signal sent through variable time delays from the local site to the remote. The rate of change of the variable time-delays with

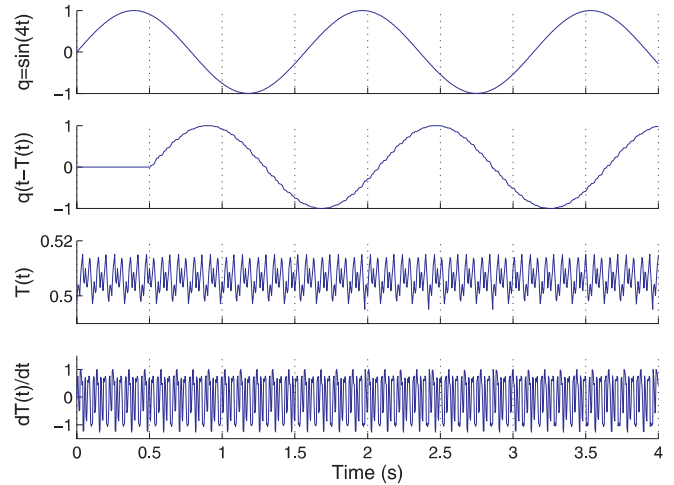


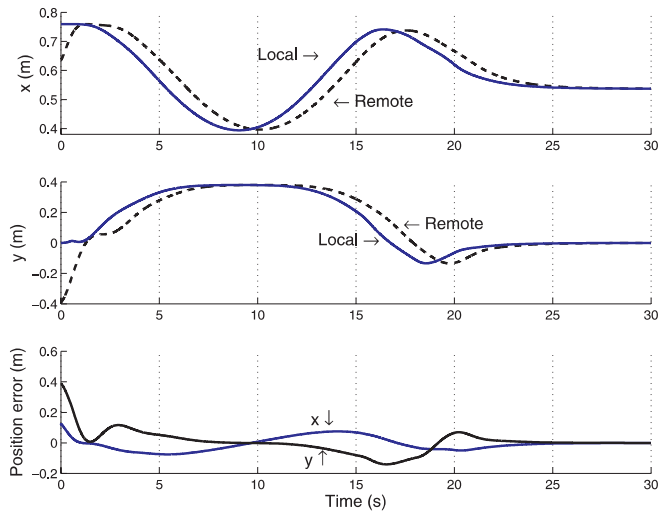
Fig. 5. Delayed signal with a variable time delay.

respect to time is always lower than or equal to one. The simulations have been carried out using MatLab SimuLink<sup>TM</sup>.

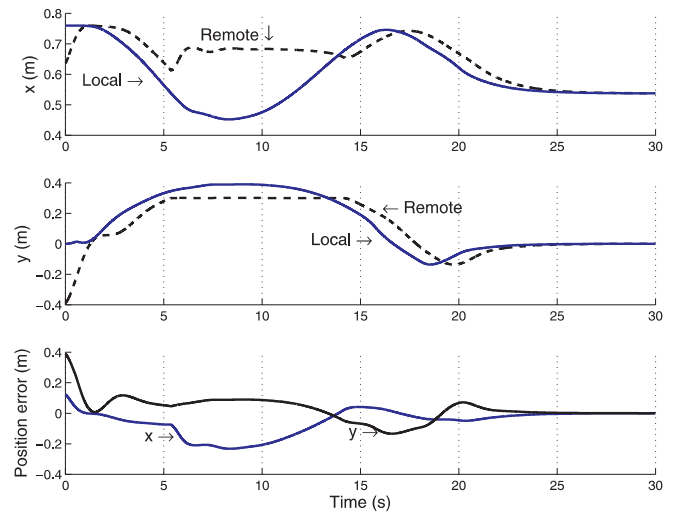
For the simulations with the P-like controller (6) the parameters used are  $*T_i = 0.55$ ,  $K_1 = 2.0$ ,  $B_1 = 0.8$ ,  $K_r = 2.8$  and  $B_r = 1.5$ , and for the PD-like controller (13),  $*T_i = 0.55$ ,  $K_1 = 2.0$ ,  $B_1 = 0.8$ ,  $K_r = 2.8$ ,  $B_r = 1.5$  and  $K_d = 0.6$ . A short calculation can show that the gains satisfy the bound (7). The initial positions for the local and remote manipulators differ one from the other, i.e.  $\mathbf{q}_l(0) = [0, 0]^T$  and  $\mathbf{q}_r(0) = [-1/9\pi, -1/8\pi]^T$ , the initial velocities and accelerations are zero. These initial conditions are the same for both controllers.

The first set of simulations have the purpose of showing that position tracking is achieved. The local and remote manipulators move freely in space, and despite the fact that both have different initial positions, when time evolves, position error goes to zero. The simulations, in cartesian space, are depicted in Figure 6(a) for the teleoperator using the P-like controller and in Figure 6(b) for the PD-like controller. It can be seen that the only difference in these signals is that position error converges faster with the P-like controller of Proposition 2.

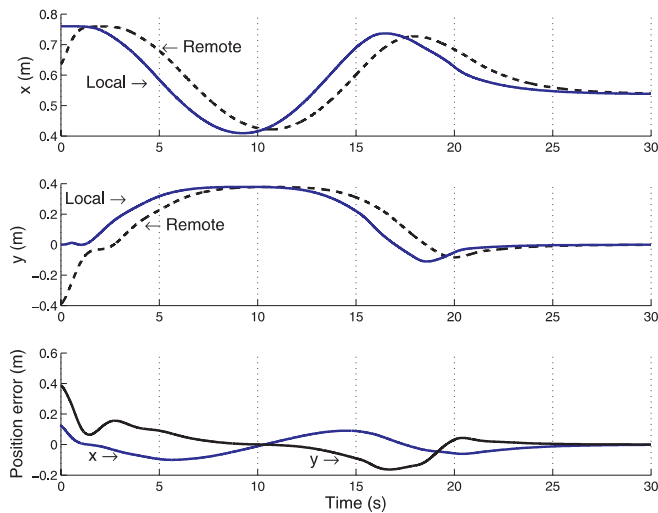
The second set of simulations aims at demonstrating the robustness of the presented schemes. It is shown that if the remote manipulator touches a high stiff wall (20,000 N m<sup>-1</sup>) the teleoperator remains stable and position tracking is also achieved. The virtual stiff wall is located at the cartesian coordinate  $y = 0.3$  m in the environment. Figure 7(a) shows the evolution of the cartesian positions for the teleoperator with the P-like controller. Around 5 seconds the remote manipulator hits the wall, and it can be noted that the  $y$  coordinate of the remote manipulator remains constant until the around 14 seconds. After that, the remote tends to follow the local manipulator and, at the end, it can be observed that position error goes to zero. The case of the teleoperator controlled by the PD-like scheme is shown in Figure 7(b). Again, the only notable differ-



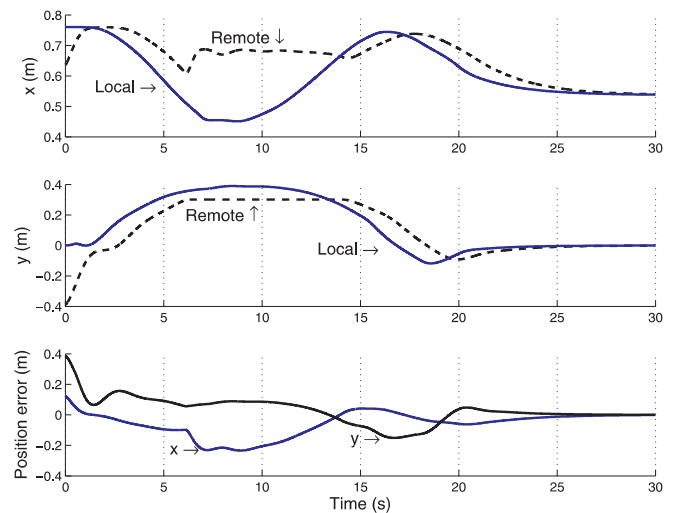
(a)



(a)



(b)



(b)

Fig. 6. Position and error in cartesian space for the teleoperator moving in free space: (a) P-like controller; (b) PD-like controller.

Fig. 7. Cartesian position and error in the presence of a stiff wall on the remote site located at 0.3 m on the y-axis: (a) P-like controller; (b) PD-like controller.

ence is that position error converges slower than the previous scheme.

in the previous simulations the controllers gains have been set such that (7) holds. The following set of simulations plots the behavior of the teleoperator when (7) does not hold. The P-like gains are set to  $K_1 = 7.8$ ,  $B_1 = 0.7$ ,  $K_r = 5.8$  and  $B_r = 1.1$ , and the same values for the PD-like with  $K_d = 0.9$ . Figure 8(a) shows the results with the P-like controller, from which an unstable behavior can be observed, and Figure 8(b) shows the results with the PD-like controller that maintains an asymptotically stable behavior of the teleoperator.

As a conclusion from these simulations it can be said that the P-like controller enables better performance when condition (7) holds, while the PD-like provides a more robust behavior when (7) does not hold, owing to, as mentioned before, the extra damping  $K_d$  injected by the PD-like controller.

## 5. Experiments

The local and remote sites were located at the Coordinated Science Laboratory (UIUC-CSL), Urbana-Champaign, IL, USA,

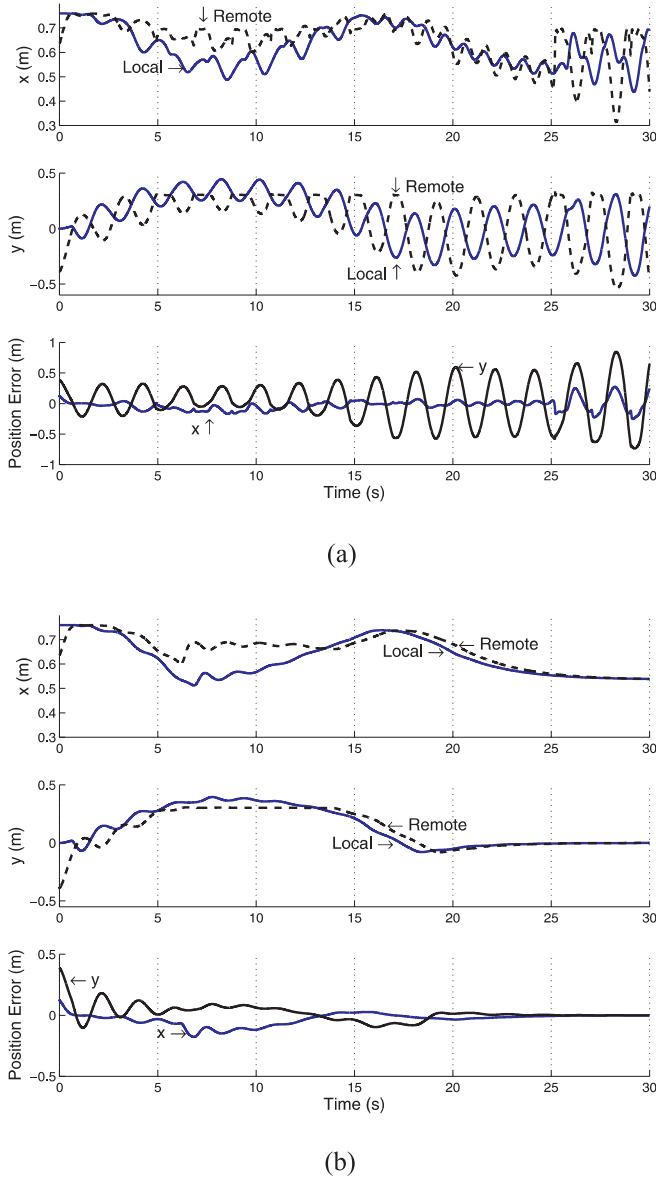


Fig. 8. Cartesian position and error of the teleoperator when condition (7) does not hold. A stiff wall is located at 0.3 m on the  $y$ -axis on the remote site: (a) P-like controller; (b) PD-like controller.

and at the Institute of Industrial and Control Engineering (UPC-IOC), Barcelona, Spain, respectively. Figure 9 shows the experimental testbed that, on the local site, mainly consists of a PHANTOM Desktop<sup>TM</sup> with six sensed DOF and three actuated DOF, and on the remote site, a six-DOF TX-90 Stäubli robot with a CS8-C<sup>TM</sup> Stäubli controller. The sites were connected through the Internet.

The interaction with the PHANTOM has been done using the educational Sensable OpenHaptics<sup>TM</sup> toolkit. The remote

robot controller was implemented using the Low Level Interface (LLI) provided by Stäubli Robotics. All software is written in C++ using sockets and POSIX threads. The graphical user interface has been developed with Trolltech's Qt library.

In order to analyze the magnitude of the time delay between the two laboratories, we sent a vector of sinusoidal signals from one laboratory to the other using a client-server application with the same payload and under the same circumstances as the robot teleoperation experiments (i.e. same hour of the day and same computers). Figure 10 shows one of these vector elements with the delay that each packet experienced to reach its destination and the time derivative of the delay. The User Datagram Protocol (UDP) has been used at a sampling rate of 4 ms, which is the sampling period of the CS8-C<sup>TM</sup> Controller at the remote site. However, the PHANTOM Desktop<sup>TM</sup> forces have been calculated at 1 ms, which is its sampling time, using a zero-order hold on the incoming signal.

Both sites' clocks were synchronized using a NTP (Network Time Protocol) server. From the results in Figure 10, the upper bound of the variable time delays is chosen as 0.3 s, for the local and remote delays (i.e.  $*T_i = 0.3$  s). There were about 2% of lost UDP packets, in each direction; out-of-sequence packets were less than 1% and have been dropped and treated as lost packets. It should be underscored that the packet payload was less than the maximum transmission unit (MTU), thus packet fragmentation has been avoided.

**Remark 2.** In the theoretical proofs of the PD-like and the scattering-based controllers, it has been assumed that the time-varying gains  $\gamma_i^2 = 1 - \dot{T}_i(t)$  are well defined. This means that the absolute value of the variable time delays is lower than the unity. However, in packet switched communications, such as the Internet, this assumption does not always hold (see Figure 10). The assumption that  $|\dot{T}_i(t)| < 1$  means that, for the sequence  $j \in \{1, 2, \dots, m\}$  for  $m < \infty$  of incoming discrete data packets with associated delays  $T_{i1}, T_{i2}, \dots, T_{im}$ , every pair of time delays has to be  $T_{ij} - T_{i,j-1} \leq \tau$  with  $\tau$  the sampling time.

In the experiments, if  $\dot{T}_i \geq 1$ , then  $\gamma_i$  is forced to zero. Switching between  $\gamma_i^2 = 1 - \dot{T}_i(t)$  for  $|\dot{T}_i(t)| < 1$  and  $\gamma_i^2 = 0$  for  $|\dot{T}_i(t)| \geq 1$  is equivalent to switch from the PD-like to the P-like, with damping equal to  $B_i + K_d$  (see (13) with  $\gamma_i = 0$ ). The resulting switched system is asymptotically stable because (14) can be also used to analyze the stability of the P-like controller, thus (14) is a shared and common Lyapunov function, which is a sufficient condition for a switched system to be asymptotically stable (see (Liberzon 2003, Theorem 2.1)).

The experiments have been performed using the P- and PD-like controllers, given by (6) and (13), respectively. The control gains are set such that (7) holds. The gain values for both controllers are  $K_1 = 20$  and  $B_1 = 5$  for the local manipulator and  $K_r = 750$  and  $B_r = 200$  for the remote manipulator; for the

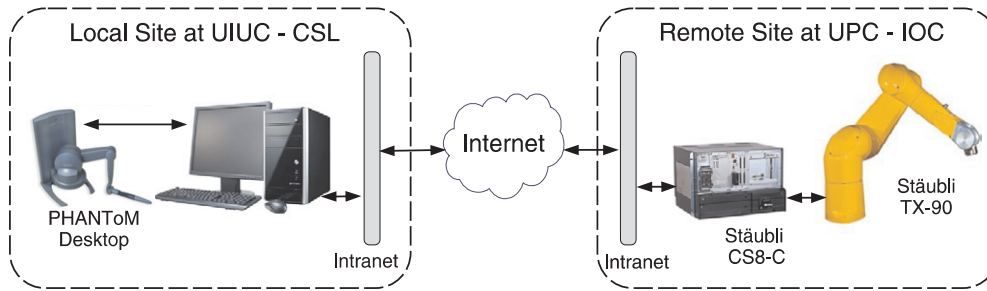


Fig. 9. The physical system.

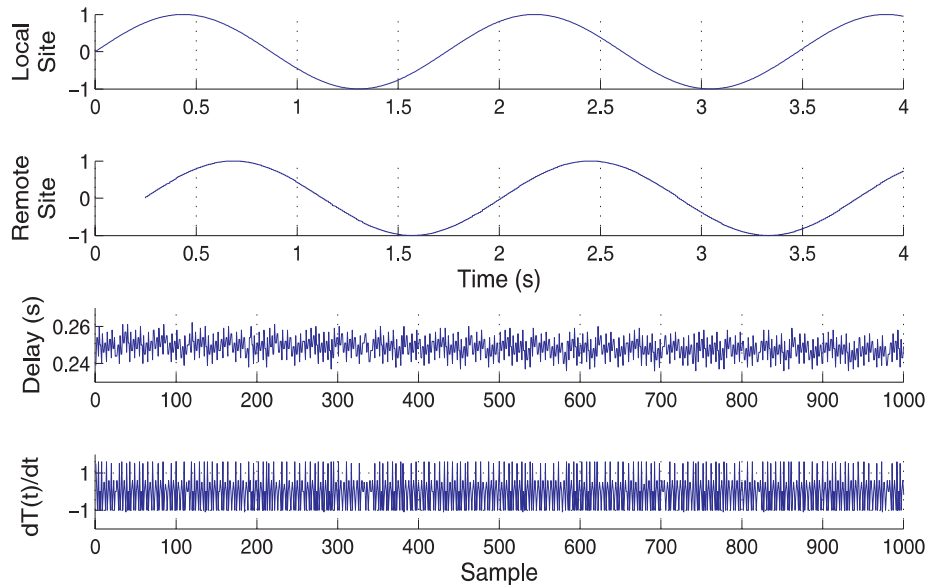


Fig. 10. Sinusoidal, sampled at 4 ms, sent from the local to the remote site.

PD-like controller  $K_d = 20$ . The experiments use only 3 DOF of each manipulator, because the PHANToM Desktop<sup>TM</sup> has only 3 actuated DOF. Figure 11 shows the experimental results for the teleoperator controlled with the P-like scheme in free space and Figure 12 depicts the articular trajectories of the teleoperator in closed loop with the PD-like controller. In both cases, the teleoperator observes a stable behavior and good position tracking performance. However, note that the simpler P-like controller provides better performance than the PD-like controller, this is mainly due to the time-varying gain  $\gamma_i$ .

The position tracking capabilities when interacting with stiff environments are presented in Figure 13, in joint space, and in Figure 14, in cartesian space. In this experiment the local and remote manipulators are controlled using the P-like scheme with the same gain values as in the free space experiments. A steel wall has been located in the remote site at  $-100$  mm on the  $z$ -axis. The human operator guides the remote manipulator to touch the steel wall in two occasions, on

the around 10 and 27 seconds. From the plots in Figures 13 and 14, it can be observed that position tracking is achieved despite stiff contacts. Position error is always bounded and it can be verified that when the remote manipulator is not interacting with the environment and the human operator does not move, the local manipulator position error asymptotically converges to zero. The experimental results of the teleoperator interacting with the steel wall and controlled by the PD-like scheme are not shown because they are similar to the results obtained with the P-like controller, confirming the simulation results presented in the previous section.

## 6. Conclusions and Future Directions

It has been proved that simple PD-like controllers, with suitably selected gains, ensure that position error remains

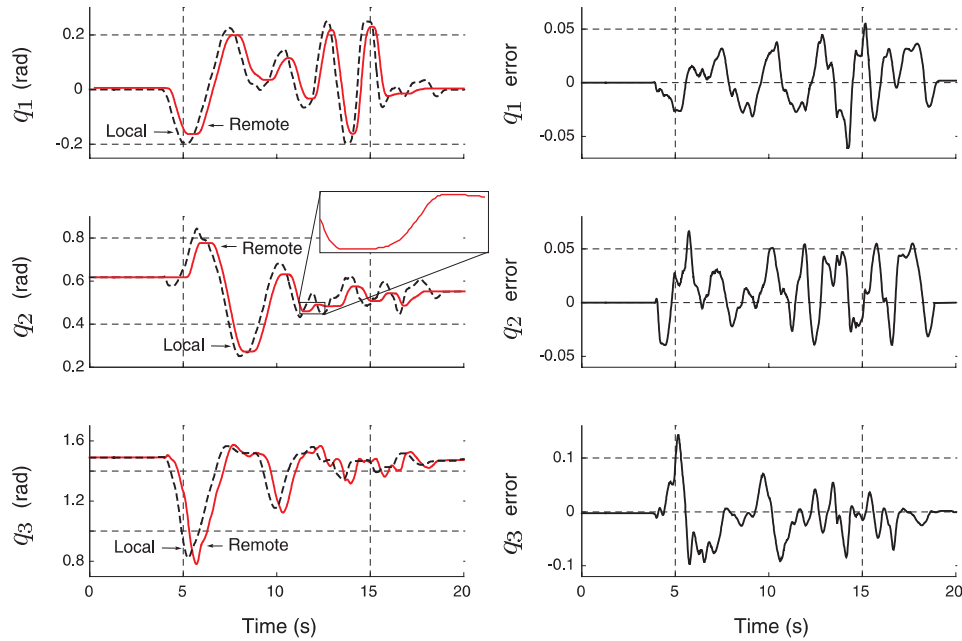


Fig. 11. Articular position and error for the teleoperator controlled by the P-like scheme in free space.

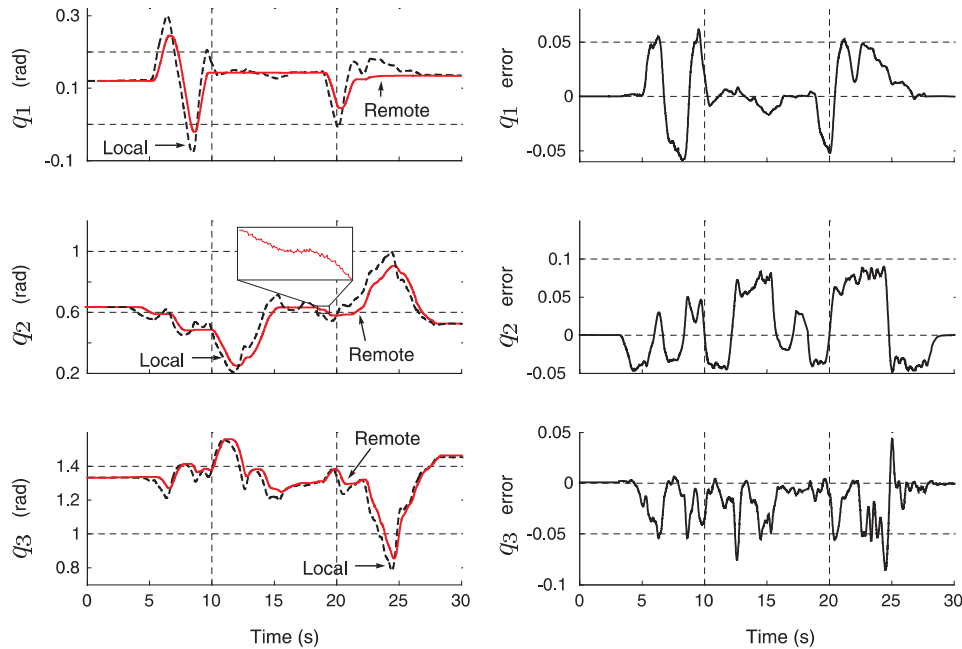


Fig. 12. Results in free space for the PD-like controller.

bounded. Furthermore, if the operator remains still and the local and remote manipulators do not enter in contact with the environment, then position error goes to zero. As shown in the proofs the key ingredient is the inclusion of damping that should “dominate” the proportional gains (see (7)) to ensure

that the velocities are in  $\mathcal{L}_2$ . Although, damping injection is instrumental for stabilization in this teleoperator application, it is not clear whether increasing it may have a deleterious effect in the system performance. For simple robot manipulators of the form (1) with performance measured via the  $\mathcal{L}_2$  gain, it

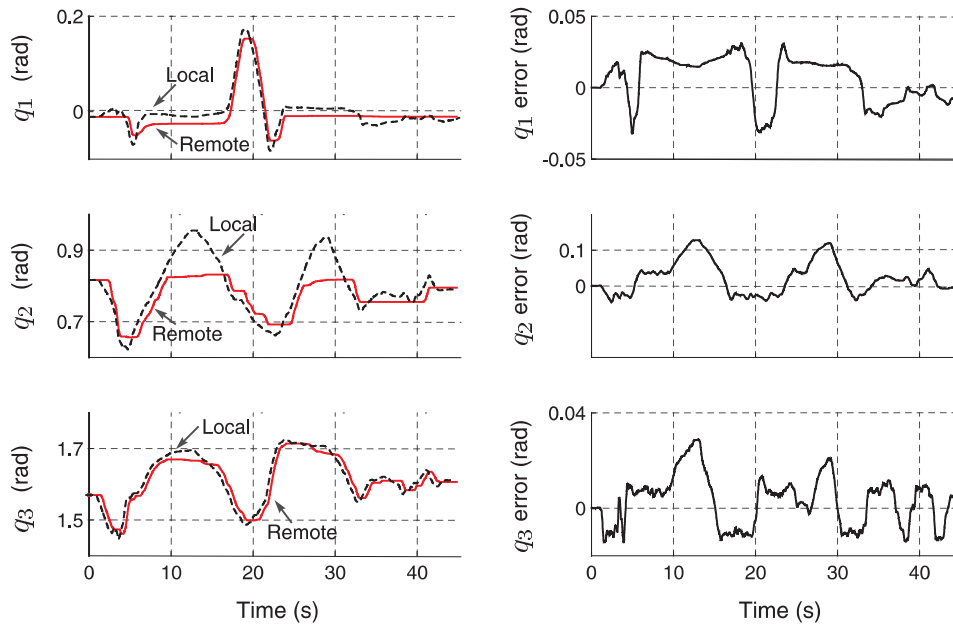


Fig. 13. Articular position and error of the teleoperator interacting with a steel wall and controlled by the P-like scheme.

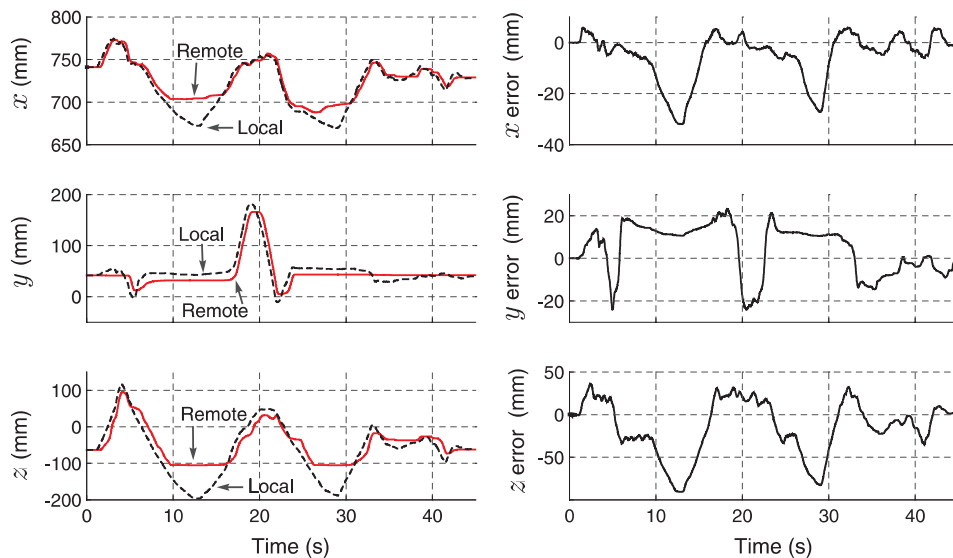


Fig. 14. Cartesian coordinates of the teleoperator interacting with a steel wall located at  $-100$  mm on the  $z$ -axis.

is shown by Scherpen and Ortega (1997) that this is indeed the case, and that, actually, there is an optimal value for the damping injection. However, most of the teleoperators are located on earth-bound or space-borne sites for which the time-delays are of the order of magnitude of hundreds of milliseconds, hence the aforementioned over-damped behaviors can be avoided.

It should be underscored that for the design of the proposed controller's gains, the upper bound of the variable time delay has to be known in advance. This assumption is not

an issue nowadays, as the time delay can be easily measured with some software tools (e.g. ping-like programs). Of course, performance will be degraded if this delay is overestimated. The effectiveness of the proposed approach has been validated through simulations and experiments. In the experiments the local and remote manipulators were separated by more than 6,000 km and communicated through the Internet with simple socket connections, for which there is no evidence suggesting disturbing effects caused by over-damped operation. The



simpler P-like controller provides better performance than the PD-like controller, because the PD-like controller includes a time-varying gain  $\gamma_i$  that downgrades performance. Tracking performance has also been experimentally validated when interacting with stiff environments.

This paper has focused on providing asymptotic zero convergence of position error for variable time delays. Future research will include the study of transient performance and rate convergence of the presented schemes. However, from the simulations and experiments it should be noted that these schemes do provide suitable transient behavior and tracking capabilities. Performance comparisons with other control schemes for variable time delay are underway and will be reported shortly.

## Acknowledgement

The authors gratefully acknowledge the comments of the anonymous reviewers: they definitely helped to improve the contents of this paper. The first author thanks the hospitality of the people at the LSS at SUPÉLEC and the CSL at UIUC, especially to Romeo Ortega and Mark W. Spong, respectively. This work has been partially supported by the Spanish CI-CYT projects: DPI2005-00112 and DPI2007-63665, the FPI program ref. BES-2006-13393, and the Mexican CONACyT grant-169003. The fourth author acknowledges the support of the Office of Naval Research under grants N00014-02-1-0011 and N00014-05-1-0186.

## Appendix: Proof of Lemma 1

**Proof.** For any vector signals  $\mathbf{a}$ ,  $\mathbf{b}$ , Schwartz's inequality is defined as

$$\int_0^t \mathbf{a}^\top(\sigma) \mathbf{b}(\sigma) d\sigma \leq \left( \int_0^t |\mathbf{a}(\sigma)|^2 d\sigma \right)^{\frac{1}{2}} \left( \int_0^t |\mathbf{b}(\sigma)|^2 d\sigma \right)^{\frac{1}{2}}$$

a direct implication is  $-\int_0^t \mathbf{a}^\top(\sigma) \mathbf{b}(\sigma) d\sigma \leq (\int_0^t |\mathbf{a}(\sigma)|^2 d\sigma)^{\frac{1}{2}} (\int_0^t |\mathbf{b}(\sigma)|^2 d\sigma)^{\frac{1}{2}}$ . On the other hand, Young's inequality for two positive numbers  $c$ ,  $d$  and any  $\alpha > 0$  is defined as  $2cd \leq \alpha c^2 + \frac{1}{\alpha} d^2$ .

Now, to prove the inequality in Lemma 1 we apply to the left-hand term of the inequality (5) first, Schwartz's (with  $\mathbf{a}(\sigma) = \mathbf{x}(\sigma)$  and  $\mathbf{b}(\sigma) = \int_{-T(\sigma)}^0 \mathbf{y}(\sigma + \theta) d\theta$ ) and then Young's inequalities, yielding

$$\begin{aligned} & -2 \int_0^t \mathbf{x}^\top(\sigma) \int_{-T(\sigma)}^0 \mathbf{y}(\sigma + \theta) d\theta d\sigma \\ & \leq \alpha \int_0^t |\mathbf{x}(\sigma)|^2 d\sigma + \frac{1}{\alpha} \int_0^t \left| \int_{-T(\sigma)}^0 \mathbf{y}(\sigma + \theta) d\theta \right|^2 d\sigma. \end{aligned} \quad (29)$$

We center our attention on finding a bound on the second term on the right-hand side of (29). Note that

$$\left| \int_{-T(\sigma)}^0 \mathbf{y}(\sigma + \theta) d\theta \right|^2 = \sum_{j=1}^n \left( \int_{-T(\sigma)}^0 y_j(\sigma + \theta) d\theta \right)^2$$

where  $y_j$  are the elements of the vector  $\mathbf{y}$ . Applying Schwartz's with  $a(\sigma) = 1$  and  $b(\sigma) = y_j(\sigma + \theta)$  we obtain

$$\begin{aligned} & \sum_{j=1}^n \left( \int_{-T(\sigma)}^0 y_j(\sigma + \theta) d\theta \right)^2 \\ & \leq T(\sigma) \sum_{j=1}^n \int_{-T(\sigma)}^0 y_j^2(\sigma + \theta) d\theta, \end{aligned}$$

which is nothing but

$$T(\sigma) \sum_{j=1}^n \int_{-T(\sigma)}^0 y_j^2(\sigma + \theta) d\theta = T(\sigma) \int_{-T(\sigma)}^0 |\mathbf{y}(\sigma + \theta)|^2 d\theta.$$

This, and the fact that  $T(\sigma) \leq *T$ , yields

$$\left| \int_{-T(\sigma)}^0 \mathbf{y}(\sigma + \theta) d\theta \right|^2 \leq *T \int_{-T(\sigma)}^0 |\mathbf{y}(\sigma + \theta)|^2 d\theta.$$

Also, note that

$$\int_{-T(\sigma)}^0 |\mathbf{y}(\sigma + \theta)|^2 d\theta \leq \int_{-*T}^0 |\mathbf{y}(\sigma + \theta)|^2 d\theta,$$

because the term inside the integral is always positive, the area on the right-hand integral is larger than or equal to the area on the left. Hence,

$$*T \int_{-T(\sigma)}^0 |\mathbf{y}(\sigma + \theta)|^2 d\theta \leq *T \int_{-*T}^0 |\mathbf{y}(\sigma + \theta)|^2 d\theta. \quad (30)$$

Replacing the bound (30) on the second right-hand term of (29) and inverting the integration order, outputs

$$\frac{*T}{\alpha} \int_{-*T}^0 \int_0^t |\mathbf{y}(\sigma + \theta)|^2 d\sigma d\theta.$$

Finally, note that  $\int_0^t |\mathbf{y}(\sigma + \theta)|^2 d\sigma = \int_{\theta}^{t+\theta} |\mathbf{y}(\sigma)|^2 d\sigma \leq \|\mathbf{y}(\sigma)\|_2^2$ ,  $\|\cdot\|_2$  is the  $\mathcal{L}_2$ -norm, defined as  $[\int_0^\infty |\mathbf{y}(\sigma)|^2 d\sigma]^{\frac{1}{2}}$ . Hence, rewriting

$$\frac{*T}{\alpha} \int_{-*T}^0 \int_0^t |\mathbf{y}(\sigma + \theta)|^2 d\sigma d\theta \leq \frac{*T}{\alpha} \int_{-*T}^0 \|\mathbf{y}(\sigma)\|_2^2 d\theta.$$

The  $\mathcal{L}_2$ -norm, in parentheses, does not depend on the integration variable  $\theta$ . Thus, the bound for the second term on the

right-hand side of (29) will finally be given by  $\frac{*T^2}{\alpha} \|y(\sigma)\|_2^2$ . Substituting this bound on (29) we obtain

$$\begin{aligned} & -2 \int_0^t \mathbf{x}^\top(\sigma) \int_{-T(\sigma)}^0 \mathbf{y}(\sigma + \theta) d\theta d\sigma \\ & \leq \alpha \int_0^t |\mathbf{x}(\sigma)|^2 d\sigma + \frac{*T^2}{\alpha} \|y(\sigma)\|_2^2. \end{aligned}$$

from which we immediately obtain (5).  $\square$

## References

- Anderson, R. and Spong, M. (1989). Bilateral control of teleoperators with time delay. *IEEE Transactions on Automatic Control*, **34**(5): 494–501.
- Arcara, P. and Melchiorri, C. (2002). Control schemes for teleoperation with time delay: a comparative study. *Robotics and Autonomous Systems*, **38**: 49–64.
- Chopra, N., Berestesky, P. and Spong, M. (2008). Bilateral teleoperation over unreliable communication networks. *IEEE Transactions on Control Systems Technology*, **16**(2): 304–313.
- Chopra, N., Spong, M., Hirche, S. and Buss, M. (2003). Bilateral teleoperation over the Internet: the time varying delay problem. *Proceedings of the 2003 American Control Conference*, Vol. 1 (Part 4), pp. 155–160.
- Chopra, N., Spong, M., Ortega, R. and Barbanov, N. (2006). On tracking performance in bilateral teleoperation. *IEEE Transactions on Robotics*, **22**(4): 844–847.
- de Rinaldis, A., Ortega, R. and Spong, M. (2006). A compensator for attenuation of wave reflections in long cable actuator–plant interconnections with guaranteed stability. *Automatica*, **42**(10): 1621–1635.
- Hirche, S. and Buss, M. (2004). Telepresence control in packet switched communication networks. *Proceedings of the IEEE International Conference on Control Applications*, pp. 236–241.
- Hokayem, P. and Spong, M. (2006). Bilateral teleoperation: an historical survey. *Automatica*, **42**: 2035–2057.
- Kelly, R., Santibáñez, V. and Loría, A. (2005). *Control of Robot Manipulators in Joint Space (Advanced Textbooks in Control and Signal Processing)*. Berlin, Springer.
- Lee, D. and Spong, M. (2006). Passive bilateral teleoperation with constant time delay. *IEEE Transactions on Robotics*, **22**(2): 269–281.
- Liberzon, D. (2003). *Switching in systems and control. Systems and Control: Foundations and Applications*. Basel, Birkhäuser.
- Lozano, R., Chopra, N. and Spong, M. (2002). Passivation of force reflecting bilateral teleoperators with time varying delay. *Proceedings of Mechatronics'02*, Enschede, The Netherlands, pp. 24–26.
- Munir, S. and Book, W. (2002). Internet-based teleoperation using wave variables with prediction. *IEEE Transactions on Mechatronics*, **7**(2): 124–133.
- Munir, S. and Book, W. (2004). Control techniques and programming issues for time delayed internet based teleoperation. *ASME Journal of Dynamic Systems, Measurement and Control*, **125**(2): 205–214.
- Namerikawa, T. and Kawada, H. (2006). Symmetric impedance matched teleoperation with position tracking. *Proceedings of the 45th IEEE Conference on Decision and Control* pp. 4496–4501.
- Niemeyer, G. and Slotine, J. (1991). Stable adaptive teleoperation. *IEEE Journal of Oceanic Engineering*, **16**(1): 152–162.
- Niemeyer, G. and Slotine, J. (2004). Telemanipulation with time delays. *The International Journal of Robotic Research*, **23**(9): 873–890.
- Nuño, E., Basañez, L. and Ortega, R. (2007). Passive bilateral teleoperation framework for assisted robotic tasks. *Proceedings of the IEEE International Conference on Robotics and Automation*, pp. 1645–1650.
- Nuño, E., Ortega, R., Barabanov, N. and Basañez, L. (2008). A globally stable PD controller for bilateral teleoperators. *IEEE Transactions on Robotics*, **24**(3): 753–758.
- Ortega, R., Chopra, N. and Spong, M. (2003). A new passivity formulation for bilateral teleoperation with time delays. *Proceedings of the CNRS-NSF Workshop: Advances in Time-delay Systems*, La Defense, Paris.
- Scherpen, J. and Ortega, R. (1997). On nonlinear control of Euler–Lagrange systems: disturbance attenuation properties. *Systems and Control Letters*, **30**(1): 49–56.
- Spong, M., Hutchinson, S. and Vidyasagar, M. (2005). *Robot Modeling and Control*. New York, Wiley.
- Tanner, N. A. and Niemeyer, G. (2005). Improving perception in time-delayed telerobotics. *The International Journal of Robotics Research*, **24**(8): 631–644.
- Yokokohji, Y., Tsujioka, T. and Yoshikawa, T. (2002). Bilateral control with time-varying delay including communication blackout. *Proceedings of the Symposium on Haptic Interfaces for Virtual Environment and Teleoperator Systems*, pp. 285–292.